Electronic Materials Letters (2018) 14:387–404
https://doi.org/10.1007/s13391-018-0043-0

Reliability Issues and Solutions in Flexible Electronics Under Mechanical Fatigue

Seol-Min Yi[1] · In-Suk Choi[2] · Byoung-Joon Kim[3] · Young-Chang Joo[4]

Received: 14 December 2017 / Accepted: 9 January 2018 / Published online: 6 March 2018

Abstract
Flexible devices are of significant interest due to their potential expansion of the application of smart devices into various fields, such as energy harvesting, biological applications and consumer electronics. Due to the mechanically dynamic operations of flexible electronics, their mechanical reliability must be thoroughly investigated to understand their failure mechanisms and lifetimes. Reliability issue caused by bending fatigue, one of the typical operational limitations of flexible electronics, has been studied using various test methodologies; however, electromechanical evaluations which are essential to assess the reliability of electronic devices for flexible applications had not been investigated because the testing method was not established. By employing the in situ bending fatigue test, we has studied the failure mechanism for various conditions and parameters, such as bending strain, fatigue area, film thickness, and lateral dimensions. Moreover, various methods for improving the bending reliability have been developed based on the failure mechanism. Nanostructures such as holes, pores, wires and composites of nanoparticles and nanotubes have been suggested for better reliability. Flexible devices were also investigated to find the potential failures initiated by complex structures under bending fatigue strain. In this review, the recent advances in test methodology, mechanism studies, and practical applications are introduced. Additionally, perspectives including the future advance to stretchable electronics are discussed based on the current achievements in research.

Keywords Reliability · Flexible · Fatigue · Bending test

1 Introduction

Flexible devices, including flexible displays, batteries, and sensors, are attracting much interest for next-generation smart electronics [1–13]. Various experimental and theoretical studies have been conducted, resulting in the competitive announcement of prototype flexible displays and batteries. Nevertheless, for commercialization, there is still a large gap between the requirements of these applications and the development of flexible electronics regarding their functionality, productivity and reliability.

Flexibility is imparted to conventional rigid electronics, which are generally fabricated on a Si wafer or glass substrate, by "making them thin" to reduce the mechanical stress/strain evolved according to the curvature relation [14, 15]. To obtain more bendability, the rigid substrate was replaced with a polymer substrate. Polyethylene terephthalate (PET) with a high transparency or polyimide (PI) with high thermal and chemical stability is generally adopted as a flexible substrate while a transparent PI film with high optical transparency and high thermal stability is currently

✉ Byoung-Joon Kim
bjkim@anu.ac.kr

✉ Young-Chang Joo
ycjoo@snu.ac.kr

[1] Research Institute of Advanced Materials, Seoul National University, 1 Gwanak-ro, Gwanak-gu, Seoul 08826, Republic of Korea

[2] High Temperature Energy Materials Research Center, Korea Institute of Science and Technology (KIST), Seoul 136791, Republic of Korea

[3] Materials Research Centre for Energy and Clean Technology, School of Materials Science and Engineering, Andong National University, 1375 Gyeongdong-ro, Andong-si, Gyeongsangbuk-do, Andong 36729, Republic of Korea

[4] Department of Materials Science and Engineering, Seoul National University, 1 Gwanak-ro, Gwanak-gu, Seoul 08826, Republic of Korea

under development. As these polymer substrates are very weak against heat compared to Si and glass, the maximum temperature of the fabrication process is restricted by the polymer substrate such that conventional materials used in electronics may not be applicable or fully functioned. Therefore, a huge amount of effort has been devoted to developing new materials and new processes to open a new era of flexible devices.

A characteristic of flexible electronics is their closeness to users. Epidermal and wearable electronics are designed to contact the human body. Thus, the reliability of flexible electronics is a very important issue because the failure of flexible electronics can cause safety problems, as well as operational malfunctions. Moreover, with the development of modern technologies, such as the internet of things (IoT), the influence of single electronic devices can cause the failure of a whole system as opposed to only individual home appliances. Regarding reliability, the most significant difference in the operational conditions of conventional electronics and flexible devices is that repeated mechanical deformations, such as bending or folding, will be continuous and will result in mechanical stress directly on the flexible electronics. Until now, the conventional electronics have been designed and produced mostly with the assumption of mechanically static operations, i.e., no repeated movements and impacts except for unintentional accidents. Thus, the electrical operational conditions and process conditions are more critical to determine the reliability of conventional electronics, such as stress migration [16, 17], electromigration [18–22], and dielectric breakdown [23, 24]. In contrast, flexible electronics suffers additional reliability issue that is caused by the mechanically dynamic operations. Current studies on flexible devices heavily focus on processes and materials developments to improve their functionality or flexibility [25–36]. However, regarding reliability assessment rudimentary bending tests were performed to demonstrate the flexibility of the developed devices without a thorough study of their electromechanical reliability. To design highly reliable flexible devices, the related studies must be carried out so that the effects of various mechanical deformations can be understood.

During the aforementioned mechanical deformation required for flexible operations, several reliability problems can occur in electronic devices [37–39]. Among those, Fatigue failure, which occurs when small deformations even below the rupture strain are repeatedly applied, is a major reliability issue closely related to long-term reliability [40–43].

In this paper, we will introduce our recent progress in bending test methods for flexible devices, and also discuss the characteristics of each test method. In the context of cyclic bending deformations, the fatigue of metallic interconnects and the subsequent degradation of electrical properties will be explained. Furthermore, methods for improving long-term reliability using nanostructures, including nanoholes, nanopores, nanowires, and multilayer structures, will be presented. Then, the last section will be devoted to the reliability of practical flexible devices implying that that the reliability study and test methods in this paper will be extended to real flexible device systems or stretchable soft materials [44–46].

2 Bending Fatigue Test Methodologies

Once flexible devices are developed, the estimation of their initial electrical performance and the evaluation of their long-term stability during mechanical deformation are required. Mechanical testing for flexible devices is slightly different from typical mechanical test methods, such as a uniaxial tensile testing or the indentation method, which aim to determine mechanical properties, for example, the yield strength and ductility [47–49]. The purpose of mechanical testing for flexible devices is to evaluate their electrical functionality, for example, the electrical resistance or carrier mobility, during or after the mechanical deformation of the sample. The applied strain due to bending deformation can be described with a simple curvature relation:

$$\varepsilon = (h_{sub} + h_{film})/2r,$$

where ε, h_{sub}, h_{film}, and $2r$ are the applied strain, substrate thickness, film thickness, and gap between the plates, respectively (r is the radius of curvature). Researchers have been developing several bending test methods that can be applied to flexible electronics.

Figure 1 shows four representative methods that are widely used for testing flexible devices: (a) the free arc bending test [50–53], (b) the variable radius bending test [54, 55], (c) the sliding plate test [56–58], and (d) the variable angle test [59, 60]. These terminologies are adopted from the international standardization [61, 62]. The free arc bending test, shown in Fig. 1a, is the most commonly used method for flexible device research. Two grips hold the edges of the sample and repeat linear motions to induce a bending motion in the target sample. For bending test methods, the method used to grip the sample is very important. The grip should be designed to avoid unintentional additional stress on the target sample near the grip so that the maximum stress will be focused at the bending point of the target sample. The electrical properties can be measured during or after the bending motion of the sample through electrical contacts at the grips. The motion of free arc bending is the simplest method, but it is difficult to induce severe bending deformation with a large bending strain. The second method is the variable radius bending test (Fig. 1b). The basic concept of the bending motion is similar to that of the free arc bending test, but the

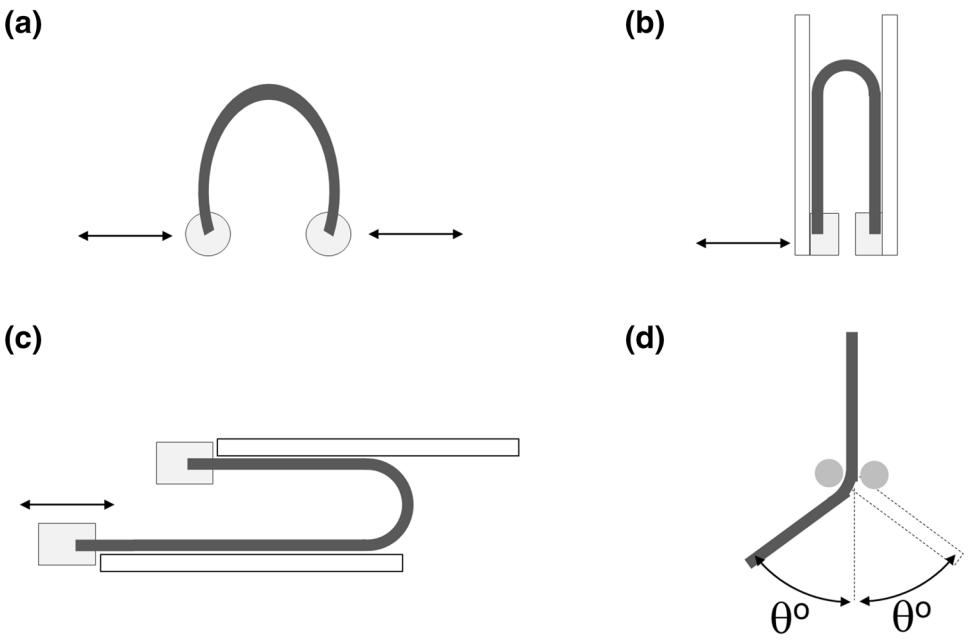

Fig. 1 Bending test methods: **a** free arc bending test, **b** variable radius bending test, **c** sliding plate test, **d** variable angle test

sample is bent between two guiding plates, which help to fit the bending shape into the target bending radius. The guiding plates enable convenient but precise control of the bending strain. The third method is the sliding plate test (Fig. 1c). The test setup is very similar to that of the variable radius bending test; however, the motion is very different. One plate is fixed, and the other plate repeats a linear motion in the direction parallel to the sample and plates. The repeated sliding motion of the plate causes local bending/unbending of the sample. The merit of this method is that the gripped part is separated from the bending part so that the connection between the grip and sample is very stable. The electrical resistance can be measured in situ using conductive grips, and multiple samples can be simultaneously tested at a high speed (~ 5 Hz). The last method is the variable angle test (Fig. 1d), where the sample is located at the center and bent to the left and right. The part of the sample subjected to bending is controlled by the round shape of the holder. Generally, the electrical properties are measured before and after mechanical deformation. As shown in Fig. 1, several kinds of bending test methods have been developed. Because each bending test represents a different bending situation, it is necessary to choose a proper bending test method that can mimic real operation conditions. In particular, additional stress near the grip should be eliminated when evaluating the reliability of the sample.

3 Fatigue Behavior of Metal Electrodes

3.1 Electrical Property Changes with the Formation of Fatigue Damage

The electrical reliability of a metal film on a polymer substrate during cyclic bending deformation was investigated using the sliding plate test. Kim et al. [56] reported the electrical resistance changes and fatigue damage morphologies, as shown in Fig. 2. A Cu film with a thickness of 1 μm was deposited on a 125 μm-thick polyimide substrate using thermal evaporation. The electrical resistance was monitored in situ during the cyclic bending deformation. Figure 2a, b show the resistance change until the completion of 5×10^5 bending cycles. During the early stage, the resistance did not change (Fig. 2b), but after a certain number of cycles, the resistance started to increase. During the late stage, the resistance increased continuously (Fig. 2a). To find the origin of the resistance increase, the surface of the sample was observed using scanning electron microscopy (SEM), as shown in Fig. 2c–f. During the early stage, no surface damage was observed (Fig. 2c), but in the sample after the electrical resistance increase had occurred, numerous cracks were observed, as shown in Fig. 2d, e. In the high magnified view (Fig. 2f), typical damage morphologies consisting of extrusions and adjacent cracks were observed, which are similar with previous reports studied using a uniaxial tensile test [43] and the beam bending test [41]. The origin of the fatigue damage in the metal was related to the dislocation motion resulting from repeated mechanical deformations. The accumulation of dislocations formed extrusions and intrusions at the

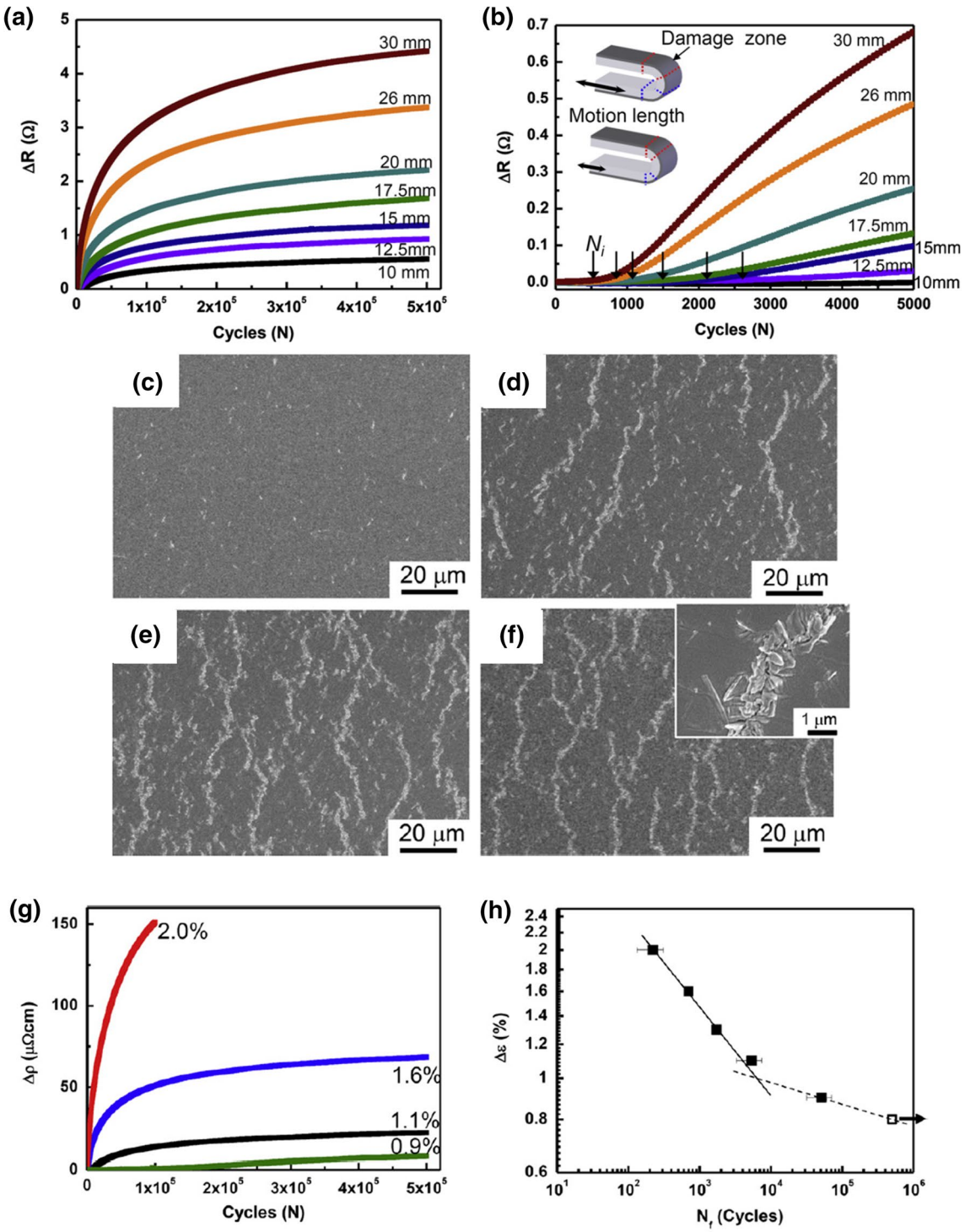

Fig. 2 Electrical resistance changes during bending fatigue during **a** the late stage and **b** the early stage. Damage morphologies after bending deformation after **c** 4×10^3, **d** 1×10^4, **e** 5×10^4, and **f** 5×10^5 bending cycles. The bending strain, linear motion length, and thickness of the Cu film were 1.1%, 10 mm, and 1 μm, respectively. **g** Resistivity changes at various bending strains from 0.9 to 2.0%. **h** Fatigue lifetime as a function of bending strain. (Reprinted with permission from Joo [56] Copyright 2012, Elsevier)

surface, which acted as stress concentration sites [63–68]. Finally, the local high stress at the fatigue damage locations caused crack evolution. Correlating the damage morphologies and the electrical resistance changes enabled the argument that the main origin of electrical resistance increase is crack formation causing electron scattering.

The electrical resistance at various bending strains is plotted in Fig. 2g. The resistance increased more and earlier for higher bending strains. The high stress accelerated the dislocation motion in the metal film; consequently, severe fatigue damage developed. To quantify the electrical lifetime, the cycle at which the electrical resistance had increased by 5% compared to the initial resistance was defined as the fatigue life time and is plotted in Fig. 2h. The fatigue lifetime decreased as the applied strain increased and can be fitted by the Coffin-Manson equation as follows

$$\frac{\Delta\varepsilon}{2} = \varepsilon_f \left(2N_f\right)^c \quad (1)$$

where $\Delta\varepsilon/2$ is the strain amplitude, ε_f is the fatigue ductility coefficient, c is the fatigue ductility exponent, and N_f is the number of cycles to failure. The fatigue lifetime can be divided into two regimes related to the elastic and plastic regimes, which are correlated to high cycle fatigue and low cycle fatigue, respectively [68–72]. Each constant was obtained by fitting the electrical lifetime. The main results are that the fatigue failure of functional electrical materials can be quantified using the electrical resistance change and that it can be predicted using a well-known fatigue equation. Furthermore, a universal equation is suggested, which can describe the electrical resistivity change after crack nucleation. This result implies that the control of crack nucleation is important to increasing the fatigue lifetime.

3.2 Film Thickness Effect on Fatigue Behavior

The mechanical and electrical properties of a metal film strongly depend on its microstructure, such as the grain size, and the film thickness. Kim et al. [57] reported the electrical reliability of metal films with various film thicknesses, as shown in Fig. 3. Cu films with various film thicknesses (200, 500 nm, and 1 μm) were prepared on a PI substrate using thermal evaporation. The monotonic fracture behaviors and long-term reliabilities of Cu films with various film thicknesses were investigated. Figure 3a shows the electrical resistance change of Cu films during the monotonic tensile test. The electrical resistance of all the samples increased following the dashed line, which was calculated by considering the increase of the sample length during the stretching of the sample. The resistance did not follow the ideal curve due to additional defect formations, such as cracks [37, 38]. The thicker Cu films (500 nm-thick film and 1 μm-thick film) showed greater stretchability compared to those of 200 nm-thick films (Fig. 3a). Figure 3b shows the mechanical stress during uniaxial tensile testing. As the film thickness decreased, the yield strength and the ultimate tensile strength (UTS) increased, but the flow stress after UTS decreased rapidly. This result implies that the mechanical strength was enhanced in the thinner films, but the ductility was reduced, which is consistent with the electrical properties during the tensile testing, as shown in Fig. 3a.

The long-term reliability of a metal film during bending fatigue was also investigated, as shown in Fig. 3c. As previously described, the electrical resistance of a Cu film increases due to fatigue damage formation during cyclic bending deformations. Interestingly, the thickness dependence varied depending on the film thickness and the applied strain. For the 200 nm-thick film, the electrical resistance did not increase for the 1.1% bending fatigue test but increased rapidly for the 2.0% bending fatigue test. In contrast, for the 1 μm-thick film, the electrical resistance kept its initial value until the 0.8% strain condition, and the fatigue failure was retarded for the 2.0% strain condition. Consequently, the thickness dependence of the fatigue lifetime varied according to the applied strain. For low strain fatigue, which corresponds to a high cycle fatigue (HCF), thinner films show longer fatigue lifetimes; however, for high strain fatigue with a low cycle fatigue (LCF), thicker films exhibit superior fatigue lifetimes (Fig. 3d). The fatigue mechanism at low strain mainly involved fatigue damage formation resulting from dislocation. The small grains in thinner films prevented dislocation motion by dislocation scarcity effect, as shown in Fig. 3b; thus crack initiation is suppressed so that the fatigue lifetime is increased. For high strain fatigue, in contrast, fracture-like failure was dominant in the thinner films so that ductile thick films with large grains exhibited longer fatigue lifetimes compared to brittle thin films. It has been known that the mechanical strength of a metal film follows the general rule of "thinner is stronger," as shown in Fig. 3b; however, the electrical reliability and lifetime of a metal film under fatigue deformation can be changed dramatically depending on the type and the magnitude of the external force, as shown in Fig. 3d. Therefore, the effect of the microstructure and operation conditions should be considered when designing highly reliable flexible electronics under fatigue deformation.

3.3 Electromechanical Behavior of Metal Lines and Films

During the application of metals in electronic devices, not only the thickness of the metallic film but also other dimensional effects must be considered for the reliability of devices. Lee et al. [73] reported the mechanical fatigue reliability of Cu interconnects on flexible substrates, as shown in Fig. 4. As shown in Fig. 4a, the electrical degradation due to bending fatigue was measured in both lines and films. Metal lines have similar dimensions to interconnects, while metal films have equivalent geometries to electrodes. By patterning thirty parallel Cu lines with widths of 8 μm, which is substantially smaller than the average crack length in a film (76.69 μm after 3×10^5 cycles, as measured from the

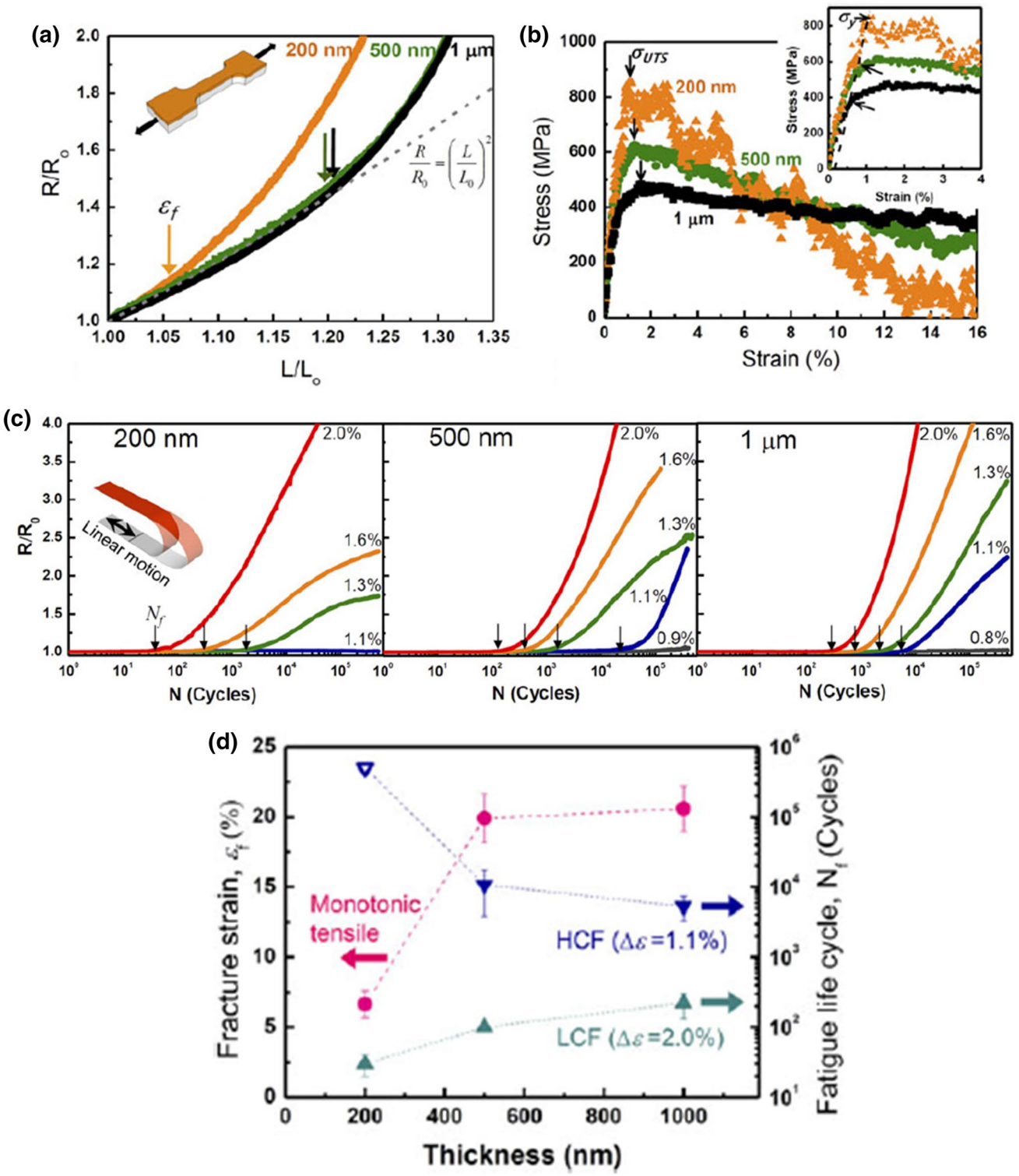

Fig. 3 **a** Electrical resistance change and **b** mechanical stress during uniaxial monotonic tensile testing of Cu films with various film thicknesses. **c** Electrical resistance change of Cu films during bending fatigue testing. **d** Fracture strain and fatigue lifetime as a function of film thickness. (Reprinted with permission from Joo [57] Copyright 2014, Cambridge University Press)

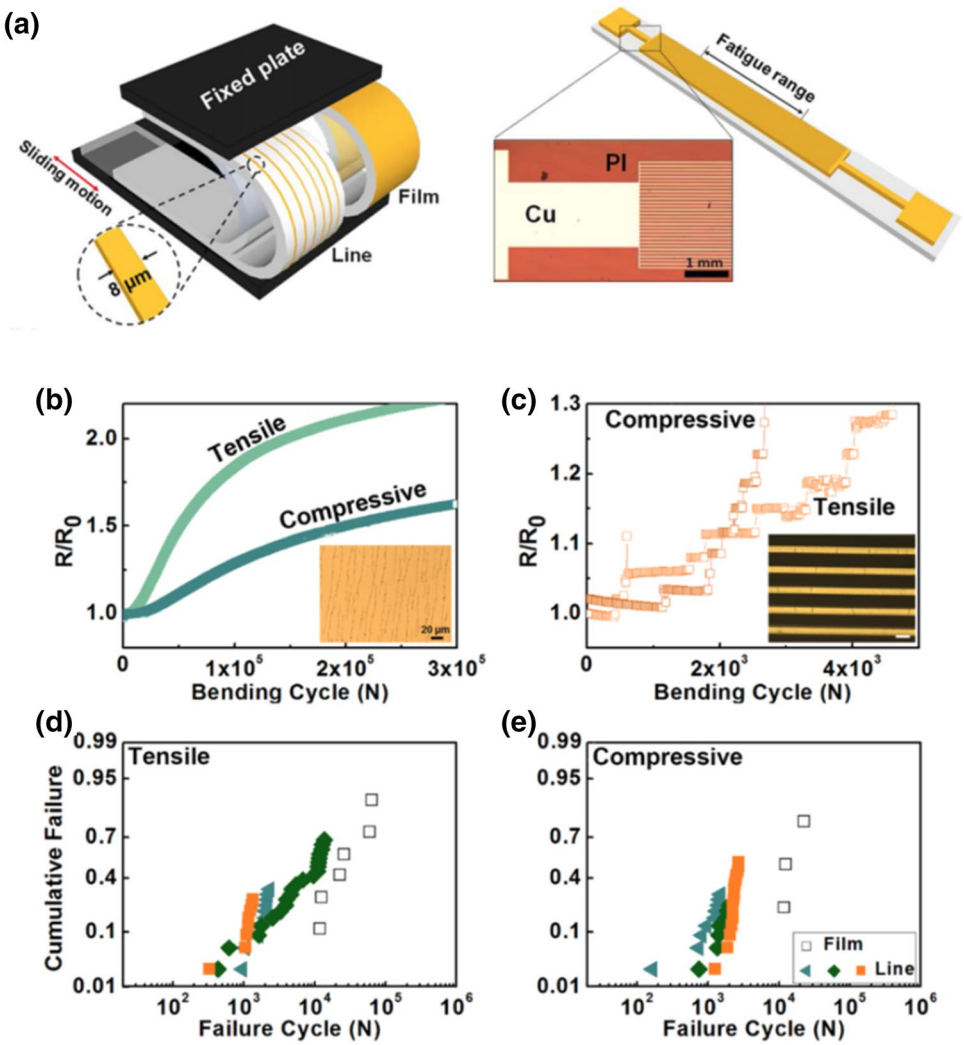

Fig. 4 **a** Schematic and resistance changes during bending fatigue testing of **b** Cu films and **c** Cu lines. Insets show the surface morphology of samples observed using an optical microscope after 3×10^5 cycles of bending. For **d** Cu films and **e** Cu lines, the lifetime when the resistance increase reaches 3% of the initial value was plotted cumulatively. (Reprinted with permission from Joo [73] Copyright 2015, KIM and Springer)

data shown in the inset of Fig. 4b) on a flexible polyimide substrate, the resistance change behavior was compared as shown in Fig. 4b, c. Regardless of the type of strain, a stepwise increase of the electrical resistance was found for metal lines, in contrast to the gradual increase found for metal films. Additionally, the size the resistance increase was similar for each step for both strain types. As noted above, both the nucleation and propagation of cracks affected the resistance increase of the films; however, cracks could propagate through the entire width of the lines immediately after crack nucleation when the line width was similar to or smaller than the crack length. Therefore, a sudden increase in the resistance could occur for metal lines. Additionally, all cracks have the same length because they were limited by the line width so that an equivalent increase, approximately 3%, was found for the occurrence of a single line fracture. It is also noteworthy that the lifetime of metal lines was shorter than that of metal films under a strain amplitude of 1%, which is expected because the strain is in the high cycle fatigue regime. The t_{50} of Cu metal lines was 6000 cycles under a tensile strain, while that of Cu metal films was 19,900 cycles under the same strain. Because data points were collected not only from early failures of metal lines but also from later failures from each step of Fig. 4c, the probabilistic error in crack nucleation can be exempted. Additionally, it is well-known that the cycles for crack growth are much smaller than those for crack nucleation in the HCF regime. Nonetheless, the effect of crack growth on lifetime under electromechanical testing should be discussed in the HCF regime because the effect of microcracks nucleated by fatigue on the electrical resistance is different from that on the mechanical properties. When a microcrack nucleated due to the electromechanical testing of the metal films, the increase of the electrical resistance was imperceptible due to how small the change in the conduction path was. Thus, more cycles are necessary to make the change of the electrical resistance distinguishable even in the HCF regime. However, for metal lines, a microcrack can induce the total fracture of single line. Consequently, the lifetimes of metal lines are shorter than those of metal films due to the lesser

number of cycles required for crack propagation. Consequently, it can be argued that the reliability of metal lines is much poorer than that of metal films. Metal layers will be patterned for the interconnects of flexible devices, and the line width and pattern size will shrink continuously as flexible devices technology evolves. Thus, the improvement of the reliability of metal lines is a very important issue to achieve fine-pitch applications.

4 Improving Long-Term Reliability by Materials Design Strategy

Recent experimental demonstrations show the improved deformability of thin films by introducing wavy, arc, or horseshoe structures [74–77], and most of the results are focused on using materials design to enhance the maximum deformability. For real industrialization, the design and fabrication of highly reliable materials are practically important because the unit materials can eventually improve the reliability of the final device system. In this section, the studies relevant to improvement of long-term reliability by materials development will be introduced.

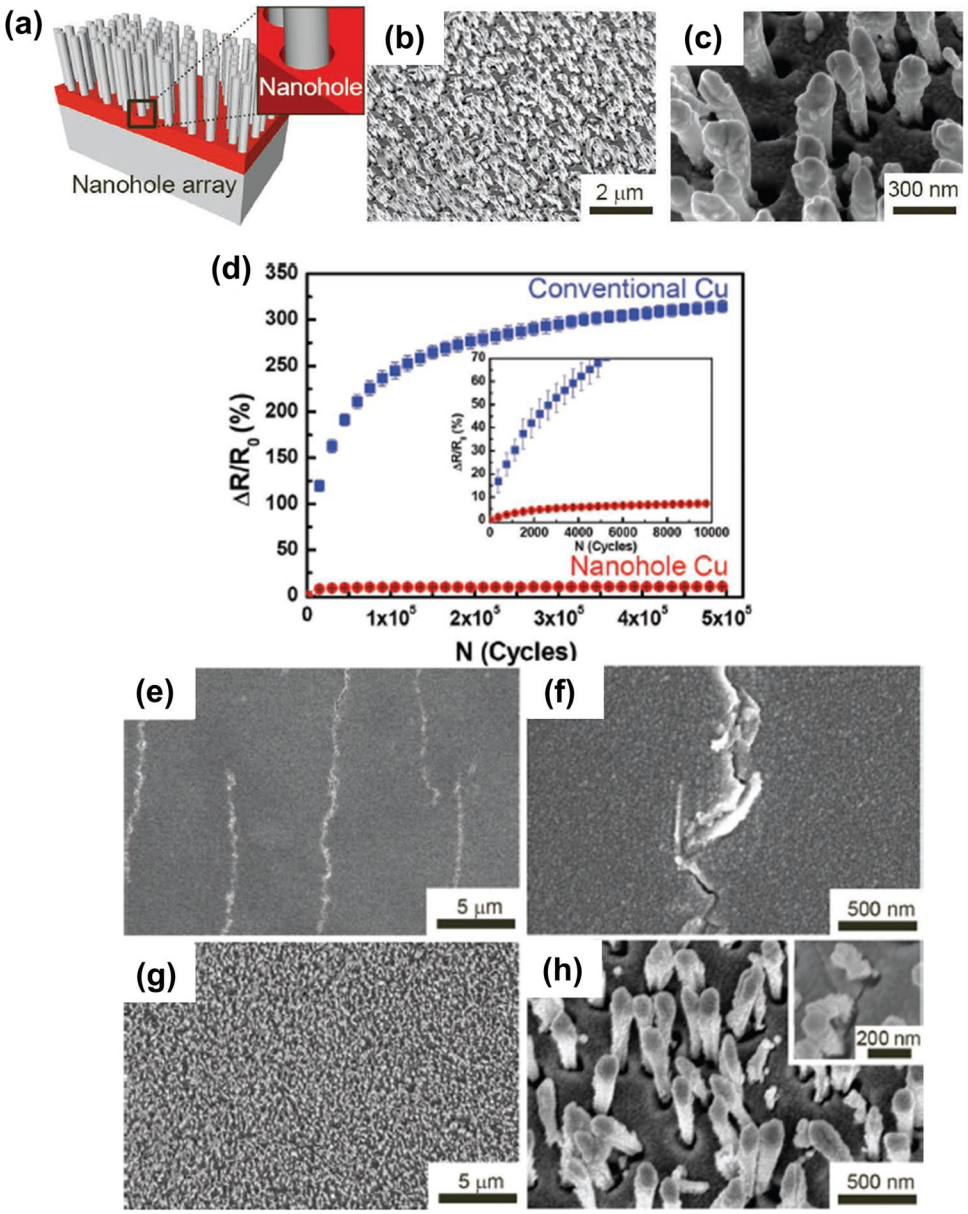

Fig. 5 **a** Schematic and **b**, **c** SEM images of a nanohole electrode. **d** Electrical resistance change of a nanohole electrode and a conventional Cu film during bending fatigue. **e**, **f** Damage morphologies after bending fatigue testing of **e**, **f** conventional Cu film and **g**, **h** nanohole electrode. (Reprinted with permission from Joo [78] Copyright 2012, Wiley)

4.1 Nanohole-Array Metal Electrodes

Typically, a hole is a defect that reduces mechanical strength and degrades electrical conductivity. However, a uniformly distributed nanohole-array can dramatically enhance long-term reliability because the nanoholes suppress defect nucleation and propagation. Kim et al. [78] demonstrated a highly reliable metal film implanted with a nanohole array, as shown in Fig. 5. Figure 5a shows a schematic of a nanohole-array electrode, which consist of a polymer substrate, a Cu layer, and nanoholes. Using plasma etching, nanorods are formed on the polymer substrate, and the metal layer is deposited on the polymer substrate. As shown in Fig. 5b, c, nanoholes are generated around the nanorods due to the shadow effect of the nanorods during the deposition process. Figure 5d shows the electrical resistance changes of the nanohole Cu and conventional Cu films. After 5×10^5 bending cycles, the electrical resistance of nanohole Cu film increased less than 7% and approximately retained its initial value, while that of the conventional Cu increased by over 300%. The surface morphologies after the bending fatigue test were observed and are presented in Fig. 5e–h. Typical fatigue damage consisting of extrusions and cracks were observed in the conventional Cu film (Fig. 5e, f). However, no fatigue damage was observed in the nanohole Cu film, as shown in Fig. 5g, h. Only short and discrete cracks were detected, as shown in the inset of Fig. 5h. The dramatic improvement of the fatigue lifetime in the nanohole Cu film can be explained in the terms of the prevention of crack nucleation and crack propagation. As previously discussed, electrical reliability during fatigue damage is directly related to crack nucleation and propagation, which are induced by local stress concentration at fatigue damage locations. Consequently, it can be argued that the origin of fatigue damage for metal film is the accumulation of dislocations. In contrast, for nanohole Cu films, the dislocation motion can be effectively distributed by nanosized holes in the metal film, and thus the formation of extrusion/intrusion can be suppressed. Therefore, crack nucleation is prevented in nanohole Cu films. Although some short cracks can form in the nanohole Cu film, the tips of the cracks are rounded. The blunting of crack tips due to nanoholes also retards crack propagation. It is notable that well-designed nanoholes can enhance long-term reliability despite the initial resistance being slightly higher than that of a conventional film.

4.2 Nanopore Inkjet-Printed Films

The development of a new process for fabricating highly reliable metal electrodes is absolutely required to increase productivity. The inkjet-printing technique has been attracting much attention as an effective method because it can produce various patterns directly on diverse flexible substrates

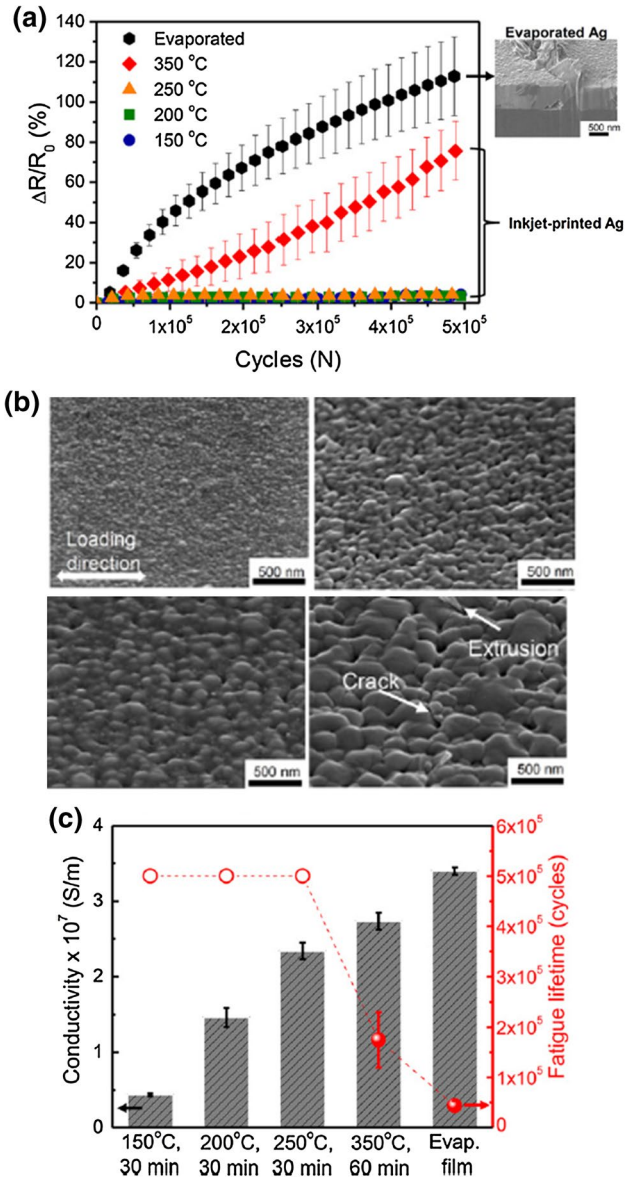

Fig. 6 **a** Electrical resistance changes of inkjet-printed electrodes with varied annealing conditions and a conventional Cu film during bending fatigue. **b** Damage morphologies of inkjet-printed electrodes with various annealing conditions after the bending fatigue test. **c** Conductivity and fatigue lifetime of inkjet-printed Ag electrodes with various annealing conditions. (Reprinted with permission from Joo [91] Copyright 2014, IOP Science)

[79–82]. To make a conductive pattern using an inkjet printing process, nanoparticle-based inks are printed on a flexible substrate, and a posttreatment is conducted. The microstructures of the printed metal electrodes depend significantly on the temperature, annealing time, and ambient conditions [83–90]. Kim et al. [91] reported the reliability change of inkjet-printed interconnects according to a thermal posttreatment, as shown in Fig. 6. The mechanical and electrical

reliability of inkjet-printed Ag electrodes was investigated after a different heat treatment.

Ag ink was inkjet printed on polymer substrates, and thermal posttreatments were conducted at 150, 200, 250, and 350 °C. The decomposition temperature of the Ag ink in this experiment was approximately 250 °C, at which the organic binders surrounding the metal nanoparticle decomposed. In the samples annealed below the decomposition temperature, small-sized nanoparticles were observed. In the samples annealed above 250 °C, necking formed between nanoparticles, and at higher temperatures, grain growth was observed. The resistance of the Ag electrodes decreased with increasing annealing temperature. Figure 6a shows the electrical resistance change of the inkjet-printed Ag electrodes for the various annealing conditions and the change of the evaporated Ag films. The samples annealed at 150, 200, and 250 °C kept their initial resistance, and no damage was observed in the surface images (Fig. 6b). However, the sample annealed at 350 °C showed an approximately 80% resistance increase. An evaporated Ag film with the same thickness as that of the inkjet-printed film was also tested. Its resistance increased by over 100%, and the typical fatigue damage consisting of extrusions and cracks was observed after the bending test. The conductivity before fatigue and the fatigue lifetime of the inkjet-printed film and the evaporated film are plotted in Fig. 6c. The initial conductivity of the inkjet-printed film increased as the annealing temperature increased, and the evaporated film exhibited the highest conductivity. In contrast, the fatigue lifetime decreased as the annealing temperature decreased, and the evaporated film showed the shortest fatigue lifetime. By correlating the resistance graph and the SEM images, it can be argued that the formation of fatigue damage was hindered in the porous structure. The nanopores in the samples that were annealed at low temperatures suppressed the accumulation of dislocation motion and the formation of fatigue damage. Fatigue damage similar to that observed in the evaporated films was observed in the sample annealed at 350 °C, which had large grains and a dense microstructure. Pores in metal electrodes are generally considered defects that impair the mechanical and electrical properties. However, controlled nanopores in inkjet-printed films can improve their long-term reliability during bending fatigue.

4.3 Metal-CNT Composite Films

Whereas nanostructures such as nanoholes and nanopores have advantages in improving the bending reliability of metal films by obstructing the motion of dislocations, annihilating vacancies, or blunting crack tips, the impairment of electrical and mechanical properties can be a collateral disadvantage in employing these nanostructures in flexible electronics. Therefore, another approach entails substituting those nanostructures with nanomaterials that have good mechanical and electrical properties, such as carbon nanotubes (CNTs). Lee et al. [89] reported improved mechanical performance for CNT and Ag nanoparticle composite films using ambient controlled annealing, as shown in Fig. 7. Figure 7a–c shows FESEM images of spin-coated Ag films and Ag/CNT films with various concentrations of CNTs. By adding CNTs into solution-based Ag films, the contacts among the Ag nanoparticles can be reinforced by the CNTs. However, the electrical resistance increases as more CNTs are added into the Ag films because of the poor interface between the CNTs and Ag. The electrical resistivity of the Ag films was 1.95 μΩcm, while that of the Ag films with 1 wt% CNTs was 2.75 μΩcm. The small contribution of the CNTs to electrical conduction can be improved using surface modification of the CNTs. Consequently, with a focus on the mechanical reliability of Ag films with CNTs, the electrical resistance as a function of cycles is plotted in Fig. 7d. In the bending fatigue test, the maximum strain was 2%, and the frequency was 1 Hz. It is interesting that a small difference in the lifetimes of the metal films was observed regardless of the amount of CNTs, considering that the failure criterion is mostly between several percent and 20%. This outcome can be affected by visible differences in the surface porosity. While a pure Ag film has a porosity of approximately 5%, Ag films with 1 and 5 wt% CNTs have porosities of ~ 7 and ~ 17%, respectively. Additionally, most interfaces between CNTs and Ag particles seem to occur at the boundaries between particles, which can also hinder the movement of dislocations. However, it is noteworthy that the electrical resistance increases more notably during crack growth (when a fatigue test was conducted for more than 10^4 cycles) as the concentration of CNTs increases. This fact can be explained by the characteristic microstructure of spin-coated Ag films. The microstructure of solution-processed films is evolved from the nanoparticle or molecules, so particulated microstructures are observed in these films. Thus, the mechanical properties and reliabilities are related closely to the contact environment among the particles within the films. CNTs in the spin-coated Ag films can restrain electrical resistance during crack growth by the reinforcement of contacts, and formation of electrical paths. As shown in Fig. 7e, f, Ag films with CNTs, shown in the images to the right (Fig. 7e), have narrower crack widths under a strain of 25% than pure Ag films, shown in the images to the left (Fig. 7f). These results imply that the lifetime under bending fatigue testing can be improved only by the retardation of crack nucleation; however, electrical degradation can be enhanced by either crack nucleation or growth.

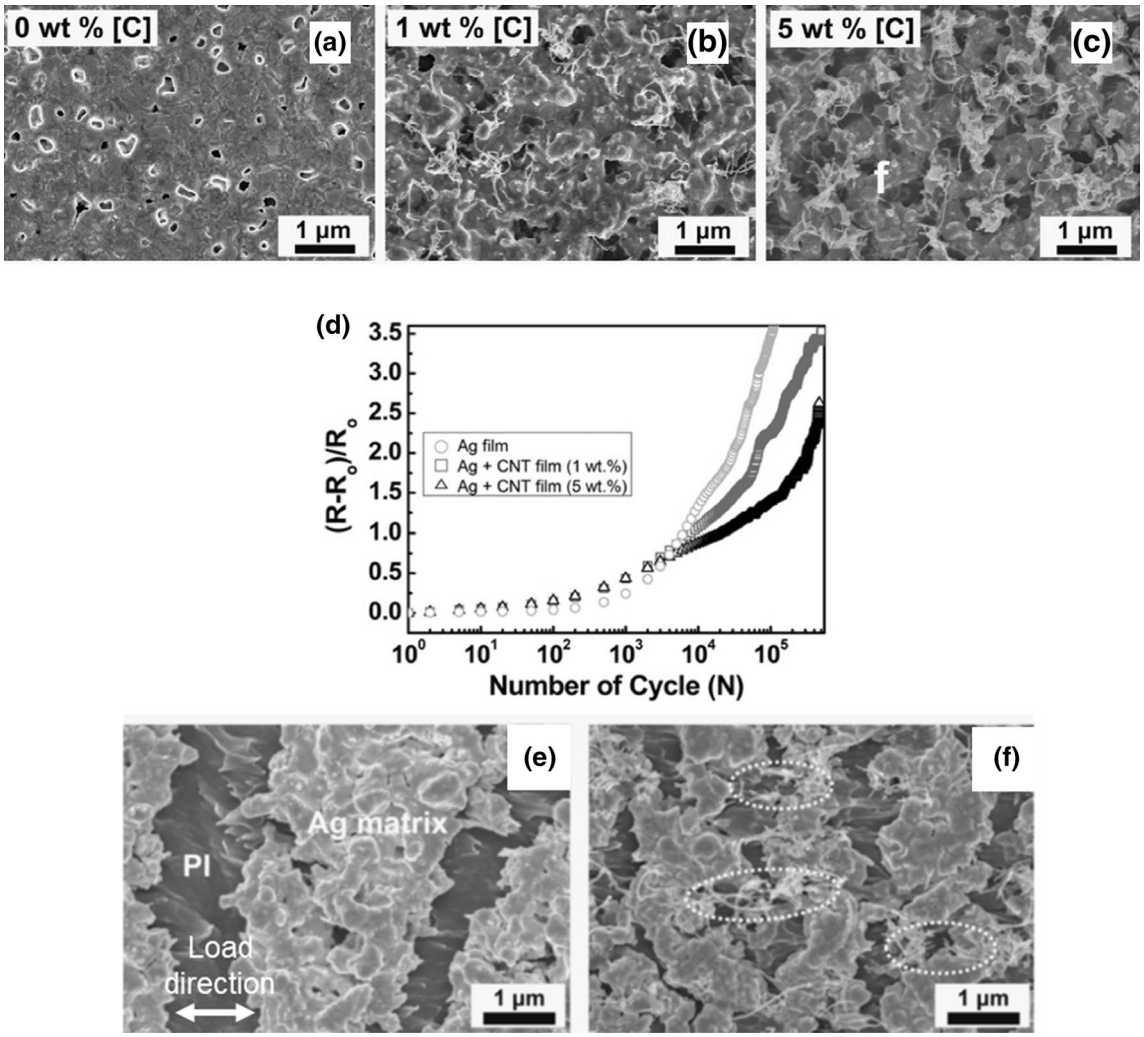

Fig. 7 FE-SEM image of **a** pure Ag, Ag with CNTs of **b** 1 wt% and **c** 5 wt% after annealing for 1 h at 250 °C. **d** The resistance changes during bending fatigue test of Ag films and Ag films with CNT. Surface morphologies of **e** pure Ag and **f** Ag films with 1 wt% CNT under strain of 25%. (Reprinted with permission from Joo [89] Copyright 2012, Elsevier)

4.4 Multilayer Metal Electrodes

In the context of the compatibility to industrial process, multilayer metal electrode structures were investigated as the most effective way to enhance the stability of metal films on polymer substrates. In particular, an underlayer is generally employed to improve the interfacial adhesion between the metal layer and the polymer film [37], and an overlayer can be adopted for passivation of the metal layer. Kim et al. [92] reported the reliability of multilayer metal films during cyclic bending deformations, as shown in Fig. 8. The electrical reliability of multilayer metal electrodes with and without an underlayer and overlayer was investigated using the bending fatigue test. For the bending test, depending on the position of the metal layer and polymer substrate, the sample can undergo either outer bending or inner bending, which implies that the metal layer is on the outside or the inside, respectively. Outer bending results in tensile stress on the metal layer, but inner bending induces compressive stress on the metal film.

Figure 8 shows the electrical resistance changes of (a) a Cu-only film, (b) a NiCr underlayer film, and (c) an Al over layer as a function of the number of bending cycles. For the Cu-only sample, the electrical resistance increased during the bending fatigue test. The resistance increment of the outer bending condition was similar to that of the inner bending test. For the NiCr underlayer sample, the electrical resistance under the outer bending condition significantly increased by over 100%, but that of the inner bending shows an approximately 20% increase. For the Al overlayer sample, the resistance increased by approximately 40% and 10% under outer bending and inner bending conditions, respectively. This finding implies that the electrical reliability

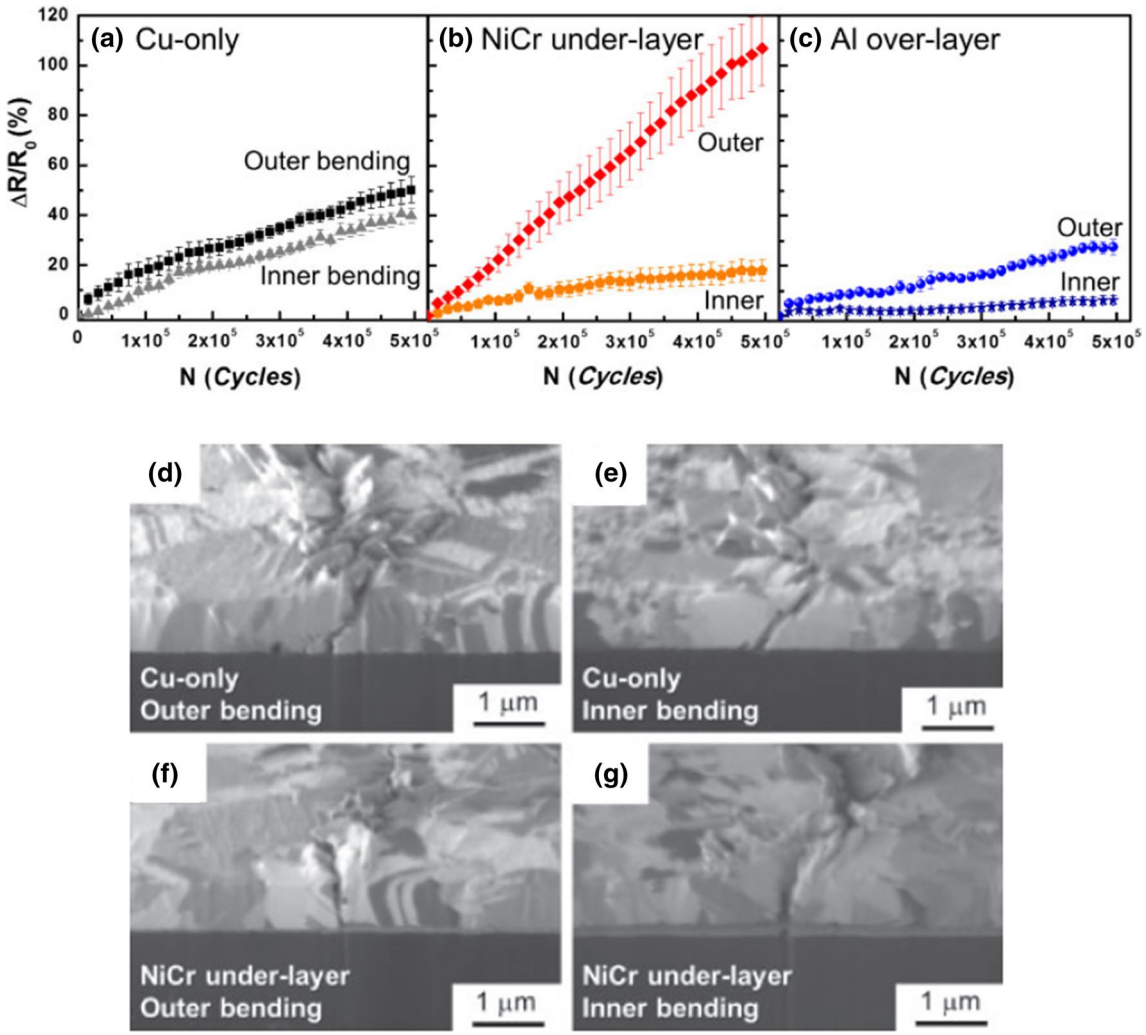

Fig. 8 Electrical resistance changes of **a** Cu-only sample, **b** Cu film with a NiCr underlayer, **c** Cu film with Al over layer. Cross-sectional images of fatigue damages of **d** Cu-only sample during outer bending, **e** Cu-only sample during inner bending, **f** Cu film with NiCr under layer during outer bending, and **g** Cu film with NiCr under layer during inner bending. (Reprinted with permission from Joo [92] Copyright 2016, IOP Science)

strongly depends on the multilayer structure of the metal film.

To determine the difference in the fatigue mechanism according to the multilayer structure, cross-sectional images of fatigue damage are presented in Fig. 8d–g. As shown in Fig. 8d, e, extrusions and cracks, which are at an approximately 45° tilt angle against the film thickness, were observed, which indicates that the fatigue damage formation that evolves by dislocation motion is the main origin of fatigue failure during both outer bending and inner bending of metal films. In contrast, for the NiCr underlayer sample, few extrusions were observed, and the direction of the cracks was vertical with respect to the film thickness. This result indicates the cracks were mainly nucleated by brittle fracture rather than extrusion/intrusion formation. Because the NiCr layer has a higher elastic modulus compared to the Cu film, the stress incompatibility near the under layer caused brittle crack nucleation.

4.5 Nanowire Metal Electrodes

A nanowire (NW) network has advantages in bending fatigue reliability. Hwang et al. [93] reported the bending reliability of an Ag NW network, which was prepared using electrostatic spraying of Ag NWs that were synthesized using the modified polyol process, as shown in Fig. 9. The changes in the electrical resistance as a function of 1% bending cycles for Ag NW networks (Fig. 9a) and the blanket Ag film (Fig. 9b) are shown. While the electrical resistance increased by approximately 80% after 5×10^5 cycles for the blanket Ag film, the resistance increased by approximately 2% after 5×10^5 cycles for the Ag NW network, as indicated

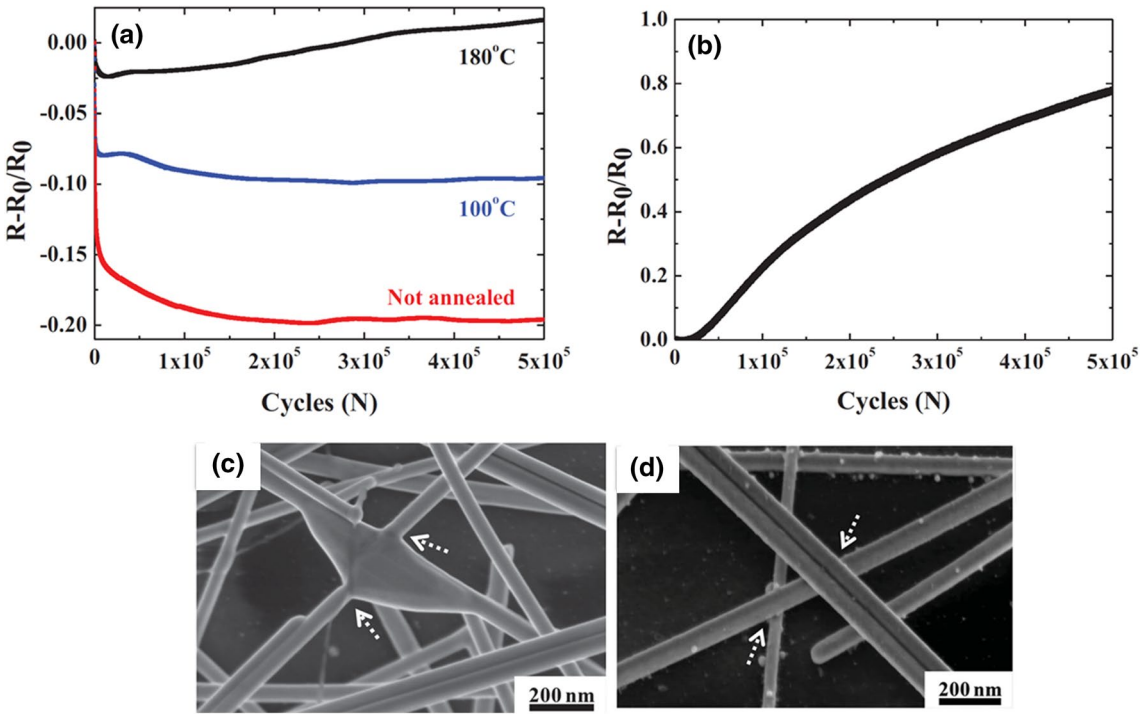

Fig. 9 Electrical resistance changes of **a** Ag NW and **b** Ag film under a bending strain of 1%. SEM observation of initial junctions among Ag NWs **a** annealed at 180 °C for 25 min and **b** not annealed before the bending fatigue test. (Reprinted with permission from Joo [93] Copyright 2014, Wiley–VCH Verlag GmbH & Co)

by the black curve. In contrast to conventional metal films, a NW network has many large spaces, which can confer transparency to the network. The movement of dislocations can be limited by the small dimension of the NWs. Additionally, if vacancies are generated by dislocation interactions over some large area, such as junctions, they can be annihilated at these spaces among the NWs. The re-orientation of NWs under strain is also helpful to enable them to endure the bending strain induced by the local release of strain through the hinge-like motion of the junctions. It should be noted that a rapid decrease was observed during the early cycles (1000–5000 cycles) of the fatigue test. Moreover, it was found that the decrease was influenced by the annealing conditions, which are independent of both the movement of dislocations and the annihilation of vacancies. From the microstructural observation shown in Fig. 9c, d, effects of annealing on the microstructure were found at the junctions between the NWs. When the NWs are annealed at a higher temperature, the junctions can be locked-in by externally induced thermal energy (Fig. 9c), in contrast to the junctions of unannealed NWs (Fig. 9d). These thermally welded junctions can reduce the electrical resistivity of the network due to their larger contact areas; however, the mechanical compensation of NWs under bending strain can also be limited several ways. Additionally, the electrical resistance of a fiber-structured material can decrease due to the re-orientation of fibers under strain. Consequently, highly reliable and transparent electrodes can be prepared with reasonable electrical properties by optimizing the microstructure of NW networks.

5 Bending Reliability of Flexible Devices

While the previous sections focused more on the reliability issue in metallic components in flexible devices, assessing the bending reliability of the entire flexible devices has also been an area of importance due to the complexity that originates from the materials and structures used. In other words, it is difficult to determine the reliability of full devices because cracks can be initiated from many possible weak points, such as interfaces, edges, and the materials themselves. Moreover, it is necessary to determine the lifetime of devices by selecting the electrical parameter that is most closely related to the functional operation of the devices under test (DUT). Here, we will describe a couple of examples from our recent results in mechanical reliability in flexible devices.

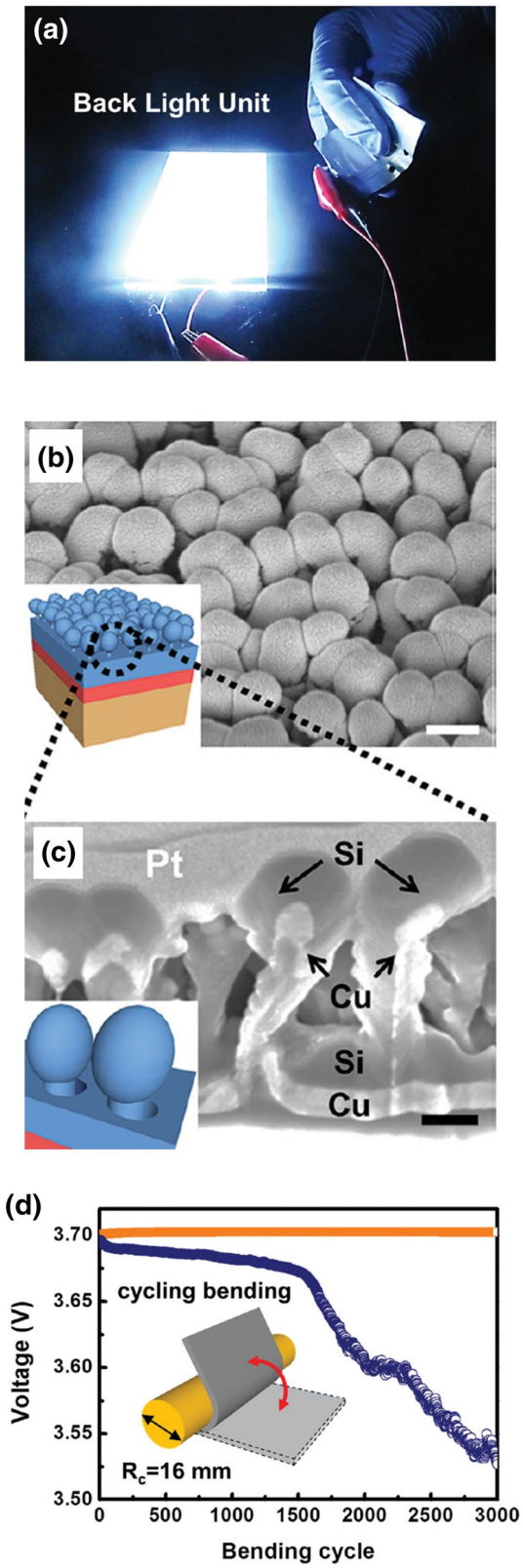

Fig. 10 **a** Bendability of Li-ion pouch cell battery with **b** nano-hairy structures for the cathode and anode. **c** Cross section of the nano-hairy structure and **d** voltage retention test during bending fatigue test at 1 Hz. (Reprinted with permission from Joo [94] Copyright 2015, Wiley–VCH Verlag GmbH & Co)

5.1 Flexible Batteries

Flexible energy applications are one of the most challenging applications for flexible electronics due to the instability that comes from the highly reactive materials contained in these devices. Particularly, using Si anodes in Flexible batteries is extremely difficult because large volume expansion during charge cycles causes interfacial delamination. However, the improved bending reliability of Li-ion batteries with Si anodes has been reported by Jung et al. [94]. The use of a nano-hairy structure (Fig. 10b, c) was suggested to improve the reliability of electrodes so that bendable Li-ion pouch cell batteries with Si anodes were successfully fabricated (Fig. 10a). After the deposition of Cu and Si on nano-hairy and flexible PI substrates that were prepared using CF_4 PECVD etching, bendable Li-ion batteries could be fabricated. As shown in the bottom of Fig. 10d, a Li-ion battery with this new structure (orange) has imperceptible changes in its output voltage during bending fatigue cycles, while a Li-ion battery with a conventional structure (blue) experiences rapid degradation after approximately 1500 bending cycles. In considering both the short lifetime compared to thin films and the poor uniformity of the Si/Cu films, the enhancement of reliability should be explained by the intrinsic improvement of the material design. It is well known that the Cu/Si interface has very poor adhesion, resulting in easy delamination as observed after the delithiation test in the same report. Therefore, the improvement of the adhesion between Cu and Si for the nano-hairy structure was attributable to the increased contact area of the hairy structure, which is closely related to the adhesion on the interface. Consequently, it can be suggested that, in contrast with thin films, extrinsic effects as well as intrinsic effects must be considered for the bending reliability of devices.

5.2 Flexible Organic Semiconductor

When the extrinsic effect is limited, the bending reliability can follow the reliability of the intrinsic materials. Various materials [95–100] and structures [101–103], which are expected to have different mechanical behaviors in comparison to conventional metals, are applied in flexible electronics as semiconductors, dielectrics and conductors. From the reports by Lee et al. [104] on the bending reliability of a simple metal–semiconductor-metal (MSM) device, which has a simple structure, it was found that the reliability of a device was determined by the reliability of the organic semiconductor. Two flexible organic semiconductors (OSC), crystalline 6,13-bis(triisopropylsilylethynyl)pentacene (TIPS-pentacene) and amorphous poly(triarylamine) (PTAA), were spin-coated on Cu combs. The comb pattern was aligned parallel to the direction of the strain, and the changes in the electrical properties were measured ex situ

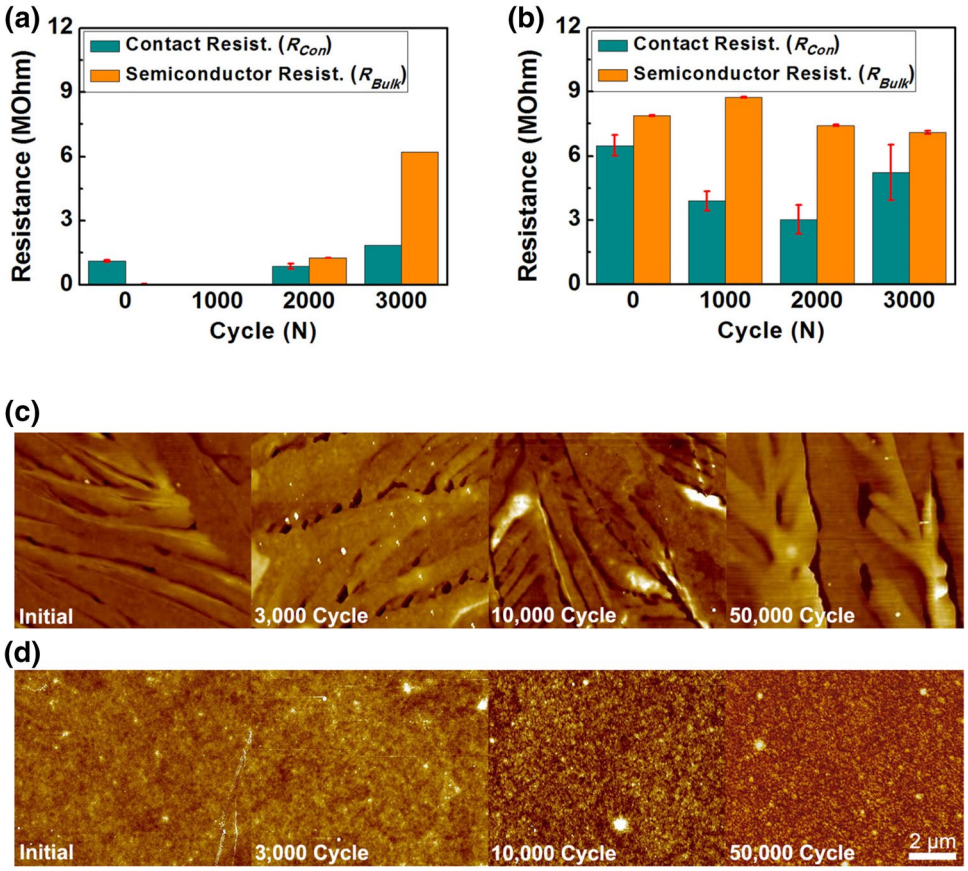

Fig. 11 Contact resistance and semiconductor resistance, calculated using the transmission-line method, of **a** TIPS-pentacene and **b** PTAA as a function of the number of bending cycles. Surface morphologies of **c** TIPS-pentacene and **d** PTAA were observed using AFM after applying bending fatigue cycles. (Reprinted with permission from Joo [104] Copyright 2013, AIP Publishing LLC)

after every thousand bending cycles. To separate the changes of the semiconductor resistance from the contact resistance, the transmission-line method was employed by changing the pitch of the combs. Figure 11a, b shows the resistances calculated from the I–V curves of the OSCs as a function of the cycle number. The initial resistance of crystalline TIPS-pentacene was smaller than one tenth that of PTAA; however, the large degradation of the semiconductor resistance was observed only at the MSM device using crystalline TIPS-pentacene. Little degradation of the contact resistance was found, i.e., the bending reliability of the OSC material determines the bending reliability of the device using the material due to the weakest link model. Thus, it can be expected that the bending reliability of films or materials must be improved to have better reliability before considering extrinsic effects. For the large degradation of TIPS-pentacene, a large difference in the surface morphology was observed using atomic force microscopy Fig. 10c, d). While amorphous PTAA showed a smooth surface without distinguishable defects, crystalline TIPS-pentacene had sharp facets (which represent the crystallinity of the material) with cavities. The mean surface roughness of PTAA and TIPS-pentacene were approximately 2–3 and 50 nm, respectively. In considering the absence of extrusions and the intergranular cracks, it can be argued that the cracks can nucleate from stress-concentrating regions, such as cavities and valleys on the surface. Therefore, amorphous OSC can be selected for some special applications that need high bending reliability, despite its poor conductivity. Otherwise, it is necessary to apply the methods described in chapter 4 (e.g., adding an over layer) to enhance the bending reliability while maintaining low electrical resistance.

Finally, the relationship between cracks and performance must also to be considered for the bending fatigue test. For example, when the crack direction is parallel to the current path, the resistance changes due to cracks are negligible. Similarly, for devices that have a vertical conduction path (e.g., OLEDs, batteries), only cracks at the electrodes and interconnects, which are the only materials related to the longitudinal current from the electrical terminal of the devices, are fatal. Thus, external effects related to vertical operation can be more important for vertical devices with highly reliable electrodes and interconnects.

6 Perspectives

Flexible electronics, which will evolve into stretchable electronics, must meet new requirements originating from their characteristic mechanical operations, as well as conventional

criteria. Bending fatigue reliability has not been previously considered in the design of conventional electronic devices; however, it is now expected to be a very important reliability criteria in flexible devices regarding the product's lifetime. Electromechanical fatigue testing is an effective method for the quantitative assessment of flexible electronics such that a great number of useful insights have been found using the method. The behavior of cracks, including nucleation and propagation, and size effects in metallic thin films on polymer substrates (e.g., film thickness and line width) have been investigated to help in the designing of reliable flexible devices. Additionally, novel ideas, mostly concerning ways to manipulate the microstructure for retarding crack initiation, have been suggested to improve the bending reliability of "flexible" passive devices. The basic understanding of the fatigue reliability of metal films has been expanded to real devices, such as Li-ion batteries and MSM devices. The reliability of flexible devices was evaluated quantitatively, and possible failure sources were discussed thoroughly.

Nevertheless, it seems that a large gap between the requirements and the mechanical properties still exists for flexible devices. Due to the low elastic compliance of flexible materials, complex and non-uniform strains can be applied to devices during even normal operations, such as unrolling and spreading. Additionally, it is difficult to improve mechanical properties and reliability without any losses in electrical performance. Thus, to pursue optimal application engineering, it is necessary to narrow the perceived gaps by utilizing several strategies such as strain engineering, test methodology, material synthesis, and finding appropriate applications. For example, the relationship among the strain components due to complex strain can be understood via the twisting fatigue reliability. New stretchable materials, which are insensitive to external strains, or meta structures, which can dissipate strain, may provide a solution to overcome practical issues in the development of flexible and stretchable electronics.

Acknowledgements This research was supported by "Development of Interconnection System and Process for Flexible Three Dimensional Heterogeneous Devices" funded by MOTIE (Ministry of Trade, Industry and Energy) and the National Research Foundation of Korea (NRF) grant funded by the Korea Government (MSIP; Ministry of Science, ICT and Future Planning) (No. 2017R1C1B5017889) in Korea.

References

1. Rogers, J.A., Bao, Z., Baldwin, K., Dodabalapur, A., Crone, B., Raju, V.R., Kuck, V., Katz, H., Amundson, K., Ewing, J., Drzaic, P.: Proc. Natl. Acad. Sci. USA **98**, 4835 (2001)
2. Khafe, A.B.M., Sakai, W., Watanabe, H., Yamauchi, H., Kuniyoshi, S., Sakai, M., Kudo, K.: Jpn. J. Appl. Phys. **53**, 05FF07 (2014)
3. Forrest, S.R.: Nature **428**, 911 (2004)
4. Lo, C.-Y., Kiitola-Keinänen, J., Huttunen, O.-H., Petäjä, J., Hast, J., Maaninen, A., Kopola, H., Fujita, H., Toshiyoshi, H.: Jpn. J. Appl. Phys. **48**, 06FC04 (2009)
5. Koo, M., Park, K.I., Lee, S.H., Jeon, D.Y., Choi, J.W., Kang, K., Lee, K.J.: Nano Lett. **12**, 4810 (2012)
6. Nam, K.T., Kim, D.W., Yoo, P.J., Meethong, N., Hammond, P.T., Chiang, Y.M., Belcher, A.M.: Science **312**, 885 (2006)
7. Li, Y., Lee, D.K., Kim, J.Y., Kim, B., Park, N.G., Kim, K., Shin, J.H., Choi, I.S., Ko, M.J.: Energy Environ. Sci. **5**, 8950 (2012)
8. Koshiba, Y., Onishi, T., Saeki, H., Misaki, M., Ishida, K., Ueda, Y.: Jpn. J. Appl. Phys. **53**, 01AB04 (2014)
9. Takano, A., Kamoshita, T.: Jpn. J. Appl. Phys. **43**, 7976 (2004)
10. Brabec, C.J.: Sol. Energy Mater. Sol. Cells **83**, 273 (2004)
11. Wagner, S., Lacour, S.P., Jones, J., Hsu, P.I., Sturm, J.C., Li, T., Suo, Z.: Physica E **25**, 326 (2004)
12. Yeo, W.-H., Kim, Y.-S., Lee, J., Ameen, A., Shi, L., Li, M., Wang, S., Ma, R., Jin, S.H., Kang, Z., Huang, Y., Rogers, J.A.: Adv. Mater. **25**, 2773 (2013)
13. Sun, J.-Y., Keplinger, C., Whitesides, G.M., Suo, Z.: Adv. Mater. **26**, 7608 (2014)
14. Suo, Z., Vlassak, J., Wagner, S.: China Particul **3**(6), 321–328 (2005)
15. Li, T., Huang, Z.Y., Xi, Z.C., Lacour, S.P., Wagner, S., Suo, Z.: Mech. Mater. **37**, 261–273 (2005)
16. Paik, J.-M., Park, Y.-J., Yoon, M.-S., Joo, Y.-C.: Scr. Mater. **48**(6), 683–688 (2003)
17. Paik, J.-M., Park, K.-C., Joo, Y.-C.: J. Electr. Mater. **133**, 48–52 (2004)
18. Joo, Y.-C., Thompson, C.V.: J. Appl. Phys. **81**(9), 6073 (1997)
19. Yoon, M.-S., Lee, S.-B., Kim, O.-H., Park, Y.-B., Joo, Y.-C.: J. Appl. Phys. **100**, 33715 (2006)
20. Yoon, M.-S., Ko, M.-K., Kim, B.-N., Kim, B.-J., Park, Y.-B., Joo, Y.-C.: J. Appl. Phys. **103**(7), 073701 (2008)
21. Yang, T.-Y., Park, I.-M., Kim, B.-J., Joo, Y.-C.: Appl. Phys. Lett. **95**, 032104 (2009)
22. Yang, T.-Y., Cho, J.-Y., Park, Y.-J., Joo, Y.-C.: Acta Mater. **60**(5), 2012–2030 (2012)
23. Hwang, S.-S., Jung, S.-Y., Joo, Y.-C.: J. Appl. Phys. **104**(4), 044511 (2008)
24. Hwang, S.-S., Jung, S.-Y., Joo, Y.-C.: J. Appl. Phys. **101**, 074501 (2007)
25. Jung, S., Lee, S., Song, M., Kim, D.-G., You, D.S., Kim, J.-K., Kim, C.S., Kim, T.-M., Kim, K.-H., Kim, J.-J., Kang, J.-W.: Adv. Energy Mater. **4**, 1300474 (2014)
26. Han, T.-H., Lee, Y., Choi, M.-R., Woo, S.-H., Bae, S.-H., Hong, B.H., Ahn, J.-H., Lee, T.-W.: Nat. Photon. **6**, 105 (2012)
27. Bonaccorso, F., Sun, Z., Hasan, T., Ferrari, A.C.: Nat. Photon. **4**, 611 (2010)
28. Eda, G., Fanchini, G., Chhowalla, M.: Nat. Nanotechnol. **3**, 270 (2008)
29. Lee, J.-Y., Connor, S.T., Cui, Y., Peumans, P.: Nano Lett. **8**, 689 (2008)
30. Krantz, J., Richter, M., Spallek, S., Spiecker, E., Brabec, C.J.: Adv. Funct. Mater. **21**, 4784 (2011)
31. De, S., Higgins, T.M., Lyons, P.E., Doherty, E.M., Nirmalraj, P.N., Blau, W.J., Boland, J.J., Coleman, J.N.: ACS Nano **3**, 1767 (2009)
32. Na, S.-I., Kim, S.-S., Jo, J., Kim, D.-Y.: Adv. Mater. **20**, 4061 (2008)
33. Kim, Y.H., Sachse, C., Machala, M.L., May, C., Muller-Meskamp, L., Leo, K.: Adv. Funct. Mater. **21**, 1076 (2011)
34. Kaltenbrunner, M., White, M.S., Glowacki, E.D., Sekitani, T., Someya, T., Sariciftici, N.S., Bauer, S.: Nat. Commun. **3**, 770 (2012)

35. Bae, S., Kim, H., Lee, Y., Xu, X., Park, J.-S., Zheng, Y., Balakrishnan, J., Lei, T., Kim, H.R., Song, Y.I., Kim, Y.-J., Kim, K.S., Ozyilmaz, B., Ahn, J.-H., Hong, B.H., Lijima, S.: Nat. Nanotechnol. **5**, 574 (2010)
36. Leem, D.-S., Edwards, A., Faist, M., Nelson, J., Bradley, D.D.C., de Mello, J.C.: Adv. Mater. **23**, 4371 (2011)
37. Lu, N., Wang, X., Suo, Z., Vlassak, J.: Appl. Phys. Lett. **91**, 221909 (2007)
38. Lu, N., Suo, Z., Vlassak, J.: Acta Mater. **58**, 1679 (2010)
39. Nix, W.D.: Metall. Trans. A **20**, 2217 (1989)
40. Schwaiger, R., Dehm, G., Kraft, O.: Philos. Mag. **83**, 693 (2003)
41. Schwaiger, R., Kraft, O.: Scr. Mater. **41**, 823 (1999)
42. Gruber, P.A., Böhm, J., Onuseit, F., Wanner, A., Spolenak, R., Arzt, E.: Acta Mater. **56**, 2318 (2008)
43. Kraft, O., Gruber, P.A., Mönig, R., Weygand, D.: Annu. Rev. Mater. Res. **40**, 293 (2010)
44. Lee, Y.-Y., Kang, H.-Y., Gwon, S.H., Choi, G.M., Lim, S.-M., Sun, J.-Y., Joo, Y.-C.: Adv. Mater. **28**, 1636 (2016)
45. Kim, C.-C., Lee, H.-H., Oh, K.H., Sun, J.-Y.: Science **353**, 682–687 (2016)
46. Sun, J.-Y., Keplinger, C., Whitesides, G.M., Suo, Z.: Adv. Mater. **26**, 7608–7614 (2014)
47. Sun, X.J., Wang, C.C., Zhang, J., Liu, G., Zhang, G.J., Ding, X.D., Zhang, G.P., Sun, J.: J. Phys. D **41**, 195404 (2008)
48. Sim, G.-D., Lee, Y.-S., Lee, S.-B., Vlassak, J.J.: Mater. Sci. Eng. A **575**, 86 (2013)
49. Sim, G.-D., Won, S., Jin, C., Park, I., Lee, S.-B., Vlassak, J.J.: J. Appl. Phys. **109**, 073511 (2011)
50. Park, M.H., Noh, M., Lee, S., Ko, M., Chae, S., Sim, S., Choi, S., Kim, H., Nam, H., Park, S., Cho, J.: Nano Lett. **14**, 4083–4089 (2014)
51. Yin, Z., Lee, C., Cho, S., Yoo, J., Piao, Y., Kim, Y.S.: Small **10**(24), 5047–5052 (2014)
52. Liang, B., Fang, L., Hu, Y., Yang, G., Zhu, Q., Ye, X.: Nanoscale **6**, 4264 (2014)
53. Abdallah, A.A., Bouten, P., With, G.: Eng. Frac. Mech. **77**(14), 2896–2905 (2010)
54. Grego, S., Lewis, J., Vick, E., Temple, D.: J. Soc. Inf. Dis. **13**(7), 575–581 (2005)
55. Ghoneim, M.T., Kutbee, A., Nasseri, F.G., Bersuker, G., Hussain, M.M.: Appl. Phys. Lett. **104**, 234104 (2014)
56. Kim, B.-J., Shin, H.-A.-S., Jung, S.-Y., Cho, Y., Kraft, O., Choi, I.-S., Joo, Y.-C.: Acta Mater. **61**, 3473 (2013)
57. Kim, B.-J., Shin, H.A.S., Lee, J.H., Yang, T.Y., Haas, T., Gruber, P.A., Choi, I.S., Kraft, O., Joo, Y.C.: J. Mater. Res. **29**, 2827 (2014)
58. Lee, Y.-J., Uk Lee, Y., Yeon, H.-W., Shin, H.-A.-S., Evans, L.A., Joo, Y.-C.: Appl. Phys. Lett. **103**, 241904 (2013)
59. Gorkhali, S.P., Cairns, D.R., Crawford, G.P.: J. Soc. Inf. Display **12**(1), 45–49 (2004)
60. Bensaid, B., Boddaert, X., Benaben, P., Gwoziecki, R., Coppard, R.: Eur. Phys. J. Appl. Phys. **55**, 23907 (2011)
61. IPC9204: Guideline on flexibility and stretchability testing for printed electronics (2016)
62. IEC 62899-202-5: Printed electronics—part 202-5: Materials—Conductive Ink—Mechanical Bending Test of a Printed Conductive Layer on a Substrate
63. Schwaiger, R., Kraft, O.: Acta Mater. **51**, 195 (2003)
64. Zhang, G.P., Volkert, C.A., Schwaiger, R., Wellner, P., Arzt, E., Kraft, O.: Acta Mater. **54**, 3127 (2006)
65. Wang, D., Volkert, C.A., Kraft, O.: Mater. Sci. Eng. A **493**, 267 (2008)
66. Zhang, G.P., Sun, K.H., Zhang, B., Gong, J., Sun, C., Wang, Z.G.: Mater. Sci. Eng. A **483**, 387 (2008)
67. Kraft, O., Schwaiger, R., Wellner, P.: Mater. Sci. Eng. A **319**, 919 (2001)
68. Sun, X.J., Wang, C.C., Zhang, J., Liu, G., Zhang, G.J., Ding, X.D.: J. Phys. D: Appl. Phys. **41**, 195404 (2008)
69. Suresh, S.: Fatigue of Materials, 2nd edn. Cambridge University Press, Cambridge (1999)
70. Dieter, G.E.: Mechanical Metallurgy. McGraw-Hill Book Company, London (1988)
71. Coffin, L.F.: Trans. ASME **76**, 931 (1954)
72. Manson, S.S.: Report, vol. 1170. Lewis Flight Propulsion Laboratory, Cleveland (1954)
73. Lee, Y.-J., Shin, H.-A.-S., Nam, D.-H., Yeon, H.-W., Nam, B., Woo, K., Joo, Y.-C.: Electron. Mater. Lett. **11**(1), 149 (2015)
74. Lacour, S.P., Wagner, S., Huang, Z., Suo, Z.: Appl. Phys. Lett. **82**, 2404 (2003)
75. Ahn, B.Y., Duoss, E.B., Motala, M.J., Guo, X., Park, S.I., Xiong, Y., Yoon, J., Nuzzo, R.G., Rogers, J.A., Lewis, J.A.: Science **323**, 1590 (2009)
76. Carta, R., Jourand, P., Hermans, B., Thoné, J., Brosteaux, D., Vervust, T., Bossuyt, F., Axisa, F., Vanfleteren, J., Puers, R.: Sens. Actuat. A **156**, 79 (2009)
77. Kim, D.H., Song, J., Won, M.C., Kim, H.S., Kim, R.H., Liu, Z., Huang, Y.Y., Hwang, K.C., Zhang, Y.W., Rogers, J.A.: Proc. Natl. Acad. Sci. USA **105**, 18675 (2008)
78. Kim, B.-J., Cho, Y., Jung, M.-S., Shin, H.-A.-S., Moon, M.-W., Han, H.N., Nam, K.T., Joo, Y.-C., Choi, I.-S.: Small **8**, 3300 (2012)
79. Ko, S.H., Pan, H., Grigoropoulos, C.P., Luscombe, C.K., Fréchet, J.M., Poulikakos, D.: Nanotechnology **18**, 345202 (2007)
80. Van OschJ, T.H.J., Perelaer, J., De Laat, A.W.M., Schubert, U.S.: Adv. Mater. **20**, 343 (2008)
81. Lee, H.M., Choi, S.Y., Kim, K.T., Yun, J.Y., Jung, D.S., Park, S.B., Park, J.: Adv. Mater. **23**, 5524 (2011)
82. H. M. Lee, S. Y. Choi, A. Jung, S. H. Ko Angew. Chem. Int. Edn. 52 7718 (2013)
83. Lee, H.H., Chou, K.S., Huang, K.C.: Nanotechnology **16**, 2436 (2005)
84. Jeong, S., Kim, D., Lee, S., Park, B.K., Moon, J.: Mol. Cryst. Liq. Cryst. **459**, 35 (2006)
85. Park, J.W., Baek, S.G.: Scr. Mater. **55**, 1139 (2006)
86. Jung, J.K., Choi, S.H., Kim, I., Jung, H.C., Joung, J., Joo, Y.C.: Philos. Mag. **88**, 339 (2008)
87. Greer, J.R., Street, R.A.: Acta Mater. **55**, 6345 (2007)
88. Kim, N.R., Lee, J.H., Yi, S.M., Joo, Y.C.: J. Electrochem. Soc. **158**, K165 (2011)
89. Lee, J.H., Kim, N.R., Kim, B.J., Joo, Y.C.: Carbon **50**, 98 (2012)
90. Yi, S.M., Lee, J.H., Kim, N.R., Oh, S., Jang, S., Kim, D., Joung, J., Joo, Y.C.: J. Electrochem. Soc. **157**, K254 (2010)
91. Kim, B.-J., Haas, T., Friederich, A., Lee, J.-H., Nam, D.-H., Binder, J.R., Bauer, W., Choi, I.-S., Joo, Y.-C., Gruber, P.A., Kraft, O.: Nanotechnology **25**, 125706 (2014)
92. Kim, B.J., Shin, H.A.S., Lee, J.H., Joo, Y.C.: Jpn. J. Appl. Phys. **55**, 06JF01 (2016)
93. Hwang, B., Shin, H.-A.-S., Kim, T., Joo, Y.-C., Han, S.M.: Small **10**(16), 3397 (2014)
94. Jung, M.-S., Seo, J.-H., Moon, M.-W., Choi, J.W., Joo, Y.-C.: Adv. Energy Mater. **5**, 1400611 (2015)
95. Lee, Y.-Y., Kang, H.-Y., Gwon, S.H., Choi, G.M., Lim, S.-M., Sun, J.-Y., Joo, Y.-C.: A strain-intensive stretchable electronic conductor: PEDOT-PSS/acrylamide organogels. Adv. Mater. **28**, 1636 (2016)
96. Kim, C.-C., Lee, H.-H., Oh, K.H., Sun, J.-Y.: Highly stretchable, transparent ionic touch panel. Science **353**, 682 (2016)
97. Kim, D.-H., Lu, N., Ghaffari, R., Rogers, J.A.: Inorganic semiconductor nanomaterials for flexible and stretchable bio-integrated electronics. NPG Asia Mater. **4**, e15 (2012)
98. Fukuda, K., Takeda, Y., Mizukami, M., Kumaki, D., Tokito, S.: Sci. Rep. **4**, 3947 (2014)

99. Root, S.E., Savagatrup, S., Printz, A.D., Rodriquez, D., Lipomi, D.J.: Chem. Rev. **117**, 6467 (2017)
100. Gupta, S.K., Jha, P., Singh, A., Chehimi, M.M., Aswal, D.K.: J. Mater. Chem. C **3**, 8486 (2015)
101. Amundson, K., Ewing, J., Kazlas, P., McCarthy, R., Albert, J.D., Zehner, R., Drzaic, P., Rogers, J., Bao, Z., Baldwin, K.: SID Symp. Digest Tech. Pap. **32**, 160 (2001)
102. Smith, D.A., Holmberg, V.C., Korgel, B.A.: ACS Nano **4**, 2356 (2010)
103. Mishra, Y.K., Kaps, S., Schuchardt, A., Paulowicz, I., Jin, X., Gedamu, D., Freitag, S., Claus, M., Wille, S., Kovalev, A., Gorb, S.N., Adelung, R.: Part. Part. Syst. Charact. **30**, 775 (2013)
104. Lee, Y.-J., Lee, Y.U., Yeon, H.-W., Shin, H.-A.-S., Evans, L.A., Joo, Y.-C.: Appl. Phys. Lett. **103**, 241904 (2013)